Melting of P wave bottomonium states in the quark-gluon plasma from lattice NRQCD

G. Aarts,[a] **C. Allton,**[a] **S. Kim,**[b] **M.P. Lombardo,**[c] **S.M. Ryan**[d] **and J.-I. Skullerud**[e]

[a] *Department of Physics, College of Science, Swansea University,*
 Singleton Park, Swansea SA2 8PP, U.K.
[b] *Department of Physics, Sejong University,*
 Seoul 143-747, Korea
[c] *INFN — Laboratori Nazionali di Frascati,*
 I-00044, Frascati (RM) Italy
[d] *School of Mathematics, Trinity College,*
 Dublin 2, Ireland
[e] *Department of Mathematical Physics, National University of Ireland Maynooth,*
 Maynooth, County Kildare, Ireland

 E-mail: g.aarts@swan.ac.uk, c.allton@swansea.ac.uk, skim@sejong.ac.kr,
 Mariapaola.Lombardo@lnf.infn.it, ryan@maths.tcd.ie,
 jonivar@thphys.nuim.ie

ABSTRACT: We study the fate of P wave bottomonium states in the quark-gluon plasma, using a spectral function analysis of euclidean lattice correlators. The correlators are obtained from lattice QCD simulations with two light quark flavours on highly anisotropic lattices, treating the bottom quark nonrelativistically. We find clear indications of melting immediately after the deconfinement transition.

Contents

1   Introduction

Ever since the suggestion that charmonium suppression may provide a signature for the formation of the quark-gluon plasma (QGP) in relativistic heavy-ion collisions [1], quarkonia (heavy quark-antiquark bound states) immersed in the QGP have been studied intensely. Due to the large energies available at the Large Hadron Collider, not only charmonium but also bottomonium can now be investigated experimentally [2–5] and this has led to an increasing theoretical interest in understanding the bottomonium system and its phenomenology at finite temperature, see e.g. the recent reviews [6–8] and references therein, as well as refs. [9–12].

In a series of papers [13–15] we have studied bottomonium at nonzero temperature using simulations of lattice QCD, in which the heavy b quarks propagate nonrelativistically through a quark-gluon plasma with $N_f = 2$ flavours. We use a highly anisotropic lattice formulation, with a total of seven different temperatures up to $2.1T_c$. In refs. [14, 15] we focused on the S waves (in the Υ and η_b channels) at zero and nonzero momentum, and found that the ground states survive up to the highest temperature available, while excited states appear to dissolve close to T_c. These results are consistent with experimental findings at the LHC [2–5]. In ref. [13] first results for P waves were presented (in the χ_b channels). In the QGP phase we observed clear indications for nonexponential decay of the euclidean lattice correlators, which was interpreted as the melting of the ground (and excited) states.

Our aim for this paper is to complete the analysis of the P wave states. In ref. [13] we studied correlators (and no spectral functions) at only four temperatures with limited statistics: here we extend this to the full ensemble also used in refs. [14, 15] and provide the spectral functions, obtained with the help of the Maximum Entropy Method (MEM). The paper is organised as follows. The correlators and spectral functions are presented in sections 2 and 3 respectively. Section 4 contains a discussion of systematics in the MEM analysis. Finally, a summary is given in section 5.

N_τ	80	32	28	24	20	18	16
$T(\text{MeV})$	90	230	263	306	368	408	458
T/T_c	0.42	1.05	1.20	1.40	1.68	1.86	2.09
N_{cfg}	250	1000	1000	500	1000	1000	1000

Table 1. Two-flavour lattice details: the lattice size is $N_s^3 \times N_\tau$ with $N_s = 12$, lattice spacing $a_s \simeq 0.162\,\text{fm}$, $a_\tau^{-1} = 7.35(3)\,\text{GeV}$, and anisotropy $a_s/a_\tau = 6$ [14].

2   Correlators

We use the formulation and lattice ensembles discussed in ref. [14] and refer to that paper for further details. Here we mention that the applicability of nonrelativistic QCD (NRQCD) [16] on the lattice [17] to treat the b quark at finite temperature is motivated by the hierarchy of effective field theories formulated in refs. [18–21]. We also emphasise that the use of NRQCD enhances the signature for quarkonium melting/survival, as it avoids several problems which have complicated the study of relativistic quarks in thermal equilibrium [22, 23]. In particular, constant contributions associated with transport and susceptibilities [24] are not present [13]. Moreover, the entire euclidean time interval can be used, due to the absence of backward moving states. For completeness, some lattice parameters are provided in table 1.

We start with a discussion of the correlators $G(\tau)$. All correlators are at zero momentum and we use point sources throughout. We have analysed P wave correlators in the $^3P_0$(scalar, χ_{b0}), $^3P_1$(axial-vector, χ_{b1}), $^3P_2$(tensor, χ_{b2}), and $^1P_1(h_b)$ channels. We found that the correlators in the different channels behave in a very similar way. To illustrate this, we show in figure 1 double ratios, namely the ratios of the correlator $G(\tau; T)$ in the χ_{b2} channel at a temperature T, normalised by the correlator at the lowest temperature, $T/T_c = 0.42$, divided by the same quantity in the χ_{b1} channel. As can be seen, the difference, although statistically significant, is at most a few per mille at the largest euclidean times. Hence from now on we present results in the χ_{b1} channel only.

In figure 2 (left) we show single ratios: the correlation functions at a given temperature T, normalized by the correlator at the lowest temperature, $T/T_c = 0.42$, as a function of the euclidean time. We observe a substantial temperature dependence in the whole temperature range. The maximal deviation, at the largest τ value for each temperature, is around 20-25%. This should be contrasted with the situation for S waves, where we found a maximal deviation of less than 3%, see figure 1 of ref. [14]. This is the first indication of strong temperature effects for P waves. We reiterate that this temperature dependence is not due to changes in the susceptibility or zero mode [23], since this contribution is absent in NRQCD.

In figure 2 (right) we show the effective masses,

$$a_\tau m_{\text{eff}}(\tau) = -\log[G(\tau)/G(\tau - a_\tau)], \tag{2.1}$$

as a function of τ. When the correlator takes the form of a sum of exponentials, the ground state will show up as a plateau at large euclidean times, provided that it is well
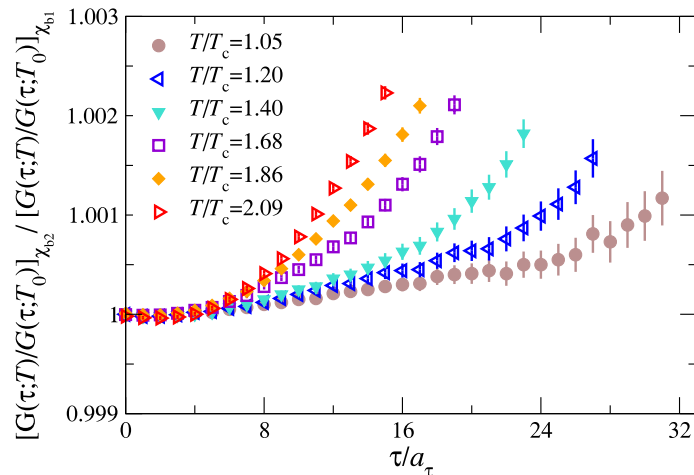
Figure 1. Ratio $[G(\tau;T)/G(\tau;T_0)]_{\chi_{b2}}$ of the correlator in the χ_{b2} channel at a given temperature T with the one at the lowest temperature, $T_0 = 0.42T_c$, divided by the same quantity in the χ_{b1} channel, $[G(\tau;T)/G(\tau;T_0)]_{\chi_{b1}}$.
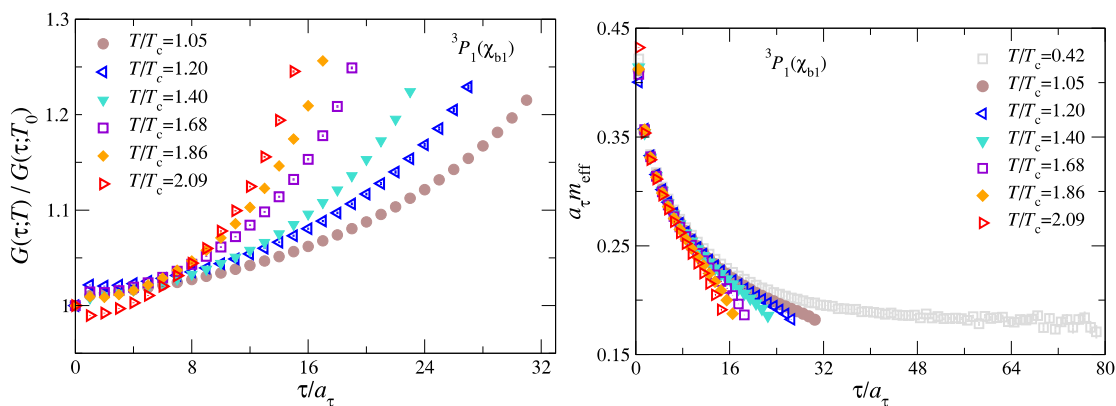

Figure 2. Left: ratio of the correlator $G(\tau;T)$ at a given temperature T with the one at the lowest temperature, $T_0 = 0.42T_c$, in the χ_{b1} channel. Right: euclidean-time dependence of the effective mass, for different temperatures.

separated from the excited states. This is indeed the case at the lowest temperature and leads to the zero-temperature spectrum discussed in refs. [13, 14]. Above T_c, we observe that the effective masses no longer follow the trend given by the correlator below T_c, but instead bend away from the low-temperature data. This implies that the spectrum has changed drastically. If isolated bound states persist, the ground state has to be much lighter and excited states cannot be well separated. A more natural explanation is that there is no exponential decay and bound states have melted, immediately above T_c. This interpretation is supported by the spectral function analysis presented next.
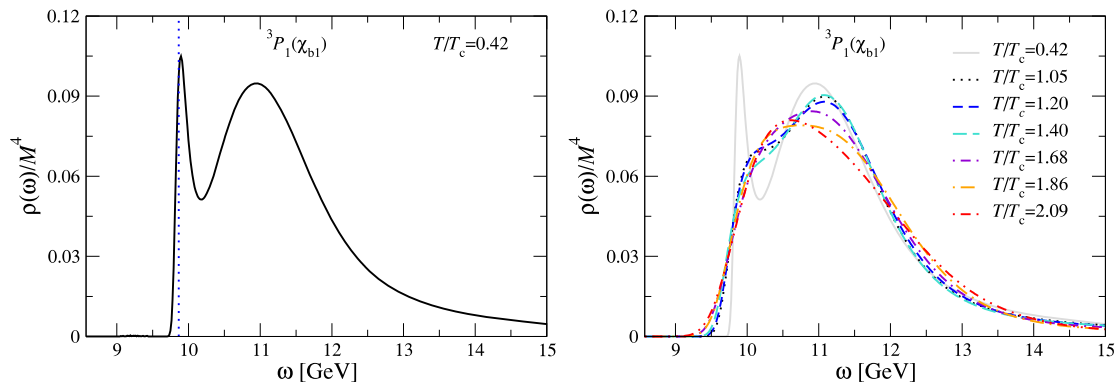
Figure 3. Spectral function in the χ_{b1} channel at the lowest temperature (left) and at all temperatures (right). The dotted line on the left indicates the position of the ground state obtained with a standard exponential fit.

3 Spectral functions

To obtain further insight into how P wave states are modified in the QGP, we now turn to a spectral-function analysis, similar to that presented in refs. [14, 15]; we refer to those papers for details. In NRQCD the spectral relation reads [13, 19]

$$G(\tau) = \int_{\omega_{\mathsf{min}}}^{\omega_{\mathsf{max}}} \frac{d\omega}{2\pi} \, K(\tau, \omega) \rho(\omega), \qquad K(\tau, \omega) = e^{-\omega\tau}, \qquad (3.1)$$

both at zero and nonzero temperature, unlike the case of relativistic quarks, where the kernel $K(\tau, \omega)$ is temperature dependent. We invert eq. (3.1) with the help of MEM [25, 26], using a constant default model, with limits $a_\tau\omega_{\mathsf{min}} \sim 0$ and $a_\tau\omega_{\mathsf{max}} \sim 2$ [14]. Since the heavy quark mass scale is integrated out, energies are determined up to an overall additive shift, which is fixed by comparing the spectrum at zero temperature with the actual physical spectrum. Specifically, we used the $\Upsilon(1S)$ mass. We therefore identify $a_\tau\omega = 0$ with $\omega = 8.57\,\mathrm{GeV}$ [14].

The result at the lowest temperature is given in figure 3 (left). The dotted vertical line indicates the mass of the lowest-energy state obtained with an exponential fit. We see from this that the narrow peak in the spectral function corresponds to the ground state. The second, wider structure is presumably a combination of excited states and lattice artefacts, see below. We note that we have not been able to extract the mass of the first excited state with an exponential fitting procedure. The spectral functions for all temperatures are shown in figure 3 (right). We find no evidence of a ground state peak for any of the temperatures above T_c. This is consistent with the interpretation of the correlator study presented above and supports the conclusion that the P wave bound states melt in the QGP.

In order to interpret the remaining structure, we compare it with the spectral function computed on the lattice, in the absence of interactions [14]. In the continuum the free spectral function in the P wave channel is given by [19]

$$\rho_P^{\mathsf{free,cont}}(\omega) \sim (\omega - \omega_0)^{3/2}\,\Theta(\omega - \omega_0), \qquad (3.2)$$
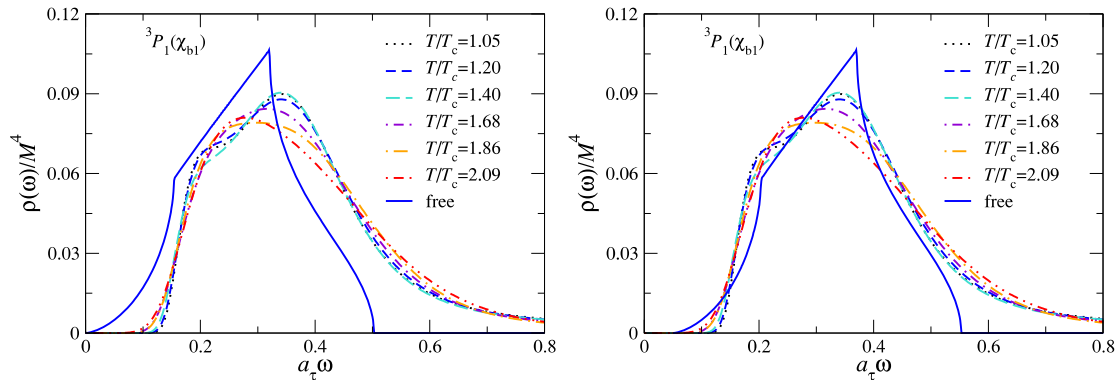
Figure 4. Comparison with the free lattice spectral function above T_c with the threshold at $a_\tau \omega = 0$ (left) and slightly shifted (right).

where ω_0 is the two-quark threshold. Note that in NRQCD the free spectral function is independent of the temperature. On the lattice this simple expression is modified due to lattice artefacts: in particular, since the lattice momenta take values in the first Brillouin zone only, it has support in a finite energy range. Moreover the edges of the Brillouin zone show up as cusps in the free lattice spectral function, see appendix A of ref. [14] for details.

In figure 4 we show the free lattice spectral functions, together with the spectral functions above T_c. In NRQCD the area under the spectral function is given by the source at $\tau = 0$ [14]; we have adjusted the overall normalisation of $\rho_P^{\rm free,lat}(\omega)$ to find approximate agreement. In principle the threshold ω_0, where $\rho_P^{\rm free,lat}(\omega)$ starts to increase, is determined by twice the heavy quark mass. In the free calculation, this coincides with $a_\tau \omega = 0$, as in figure 4 (left), but in the interacting theory this value will depend on details of the lattice simulations and the heavy quark mass, and will in general be different. Therefore we are allowed to shift $\rho_P^{\rm free,lat}(\omega)$ horizontally, as in figure 4 (right). On the other hand, what is not adjustable is the width of the region where $\rho_P^{\rm free,lat}(\omega)$ has support and the position of the cusps. Therefore these features can be sensibly compared between the interacting and the free theory: we observe that the structure of the full spectral functions from NRQCD simulations in the QGP is not too dissimilar to that of $\rho_P^{\rm free,lat}(\omega)$, another indication of unbound, quasi-free b quarks. This lends further support to the conclusion drawn in ref. [13] from an analysis of the correlators, namely that the system in the P wave channels is approaching a system of noninteracting quarks.

4 Systematics

To ensure the robustness of the results produced with MEM, it is necessary to investigate the dependence on the various input variables in the MEM analysis, such as the default model, the precision of the data and the time range used. A detailed study of systematic effects in the MEM analysis in the case of S wave channels can be found in our previous paper [14]. We have repeated that analysis for the P wave channels considered here and found that the results are again robust against variation of most of the input variables.
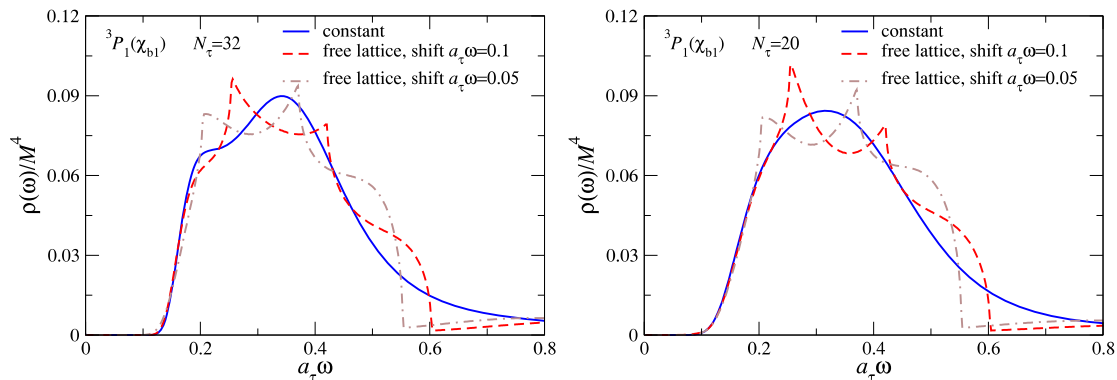
Figure 5. Reconstructed spectral functions using a constant default model and the free lattice default model, shifted by $a_\tau\omega = 0.05$ and 0.1, in the χ_{b1} channel, for $N_\tau = 32$ (left) and 20 (right).

However, we have found one aspect that is specific for the P wave channels, namely a very strong dependence on the choice of final time slice. In contrast, in the S wave channels the results do not depend strongly on the final time slice.

We start with a discussion of the default model dependence. The default model $m(\omega)$ enters in the parametrisation of the spectral function,

$$\rho(\omega) = m(\omega)\exp\sum_k c_k u_k(\omega), \tag{4.1}$$

where $u_k(\omega)$ are basis functions fixed by the kernel $K(\tau,\omega)$ and the number of time slices, while the coefficients c_k are to be determined by the MEM analysis [25]. We find that the results are insensitive to the choice of default model, provided that it is a smooth function of ω. It is also possible to use as default model the free lattice spectral function, which has cusps and support in a finite ω interval only, as shown above. To use $\rho_P^{\text{free,lat}}(\omega)$ as default model, we add a small constant so that it is nonzero in the entire ω range. We also shift it in the horizontal direction, such that the thresholds are located at $a_\tau\omega = 0.05$ and 0.1. The resulting spectral functions are shown in figure 5, together with the results from the constant default model, $m(\omega) = m_0$. We observe that the nonanalytical behaviour of the free lattice default models is still present in the reconstructed spectral functions, since the basis functions $u_k(\omega)$ are not capable of eliminating this. Shifting the default model simply results in a shift of these cusps. From this we conclude that using a lattice free default model introduces a bias which cannot be overcome. We hence favour choosing smooth default models only: the results of the previous section are obtained with a constant default model. We also see that lattice artefacts potentially set in quite close to the threshold, which can be avoided by using lattices with a finer (spatial) lattice spacing: this will be necessary to clearly separate the physical region from the region dominated by lattice artefacts. Nevertheless, we observe that the position of the threshold agrees between the three default models. Moreover, as already noted above, the spectral functions reconstructed using a constant default model have support in the region marked by the free lattice spectral function. This result seems therefore clearly encoded in the euclidean correlator data.
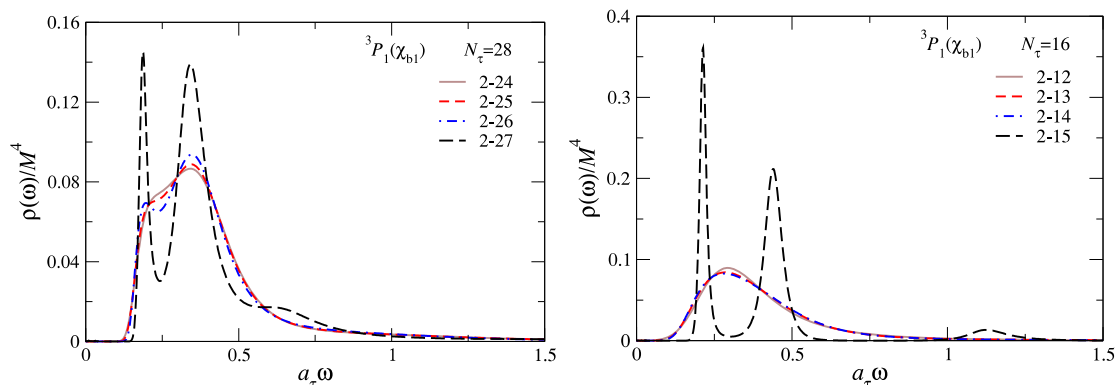
Figure 6. Dependence of the reconstructed spectral function on the final time slice used in MEM: $\tau/a_\tau \in [n_1, N_\tau - n_2]$, with $n_1 = 2$ and $n_2 = 4, 3, 2, 1$, for $N_\tau = 28$ (left) and 16 (right). The source is located at $n_1 = 0$.

We now turn to the dependence on the time range. In the MEM analysis, one chooses the time interval, which should be varied in order to establish robustness of the output. We recall that in NRQCD the correlators are not periodic in time,[1] so that in principle the entire time interval can be used, rather than only up to $\tau = 1/2T$. Thermal effects appear since the b quarks propagate through an ensemble of gluons and light quarks at finite temperature, which is implemented via the usual (anti)periodic thermal boundary conditions. Hence, even though boundary conditions do not appear explicitly in the propagation of the b quarks, they are still present indirectly through the interaction with the QGP. To test the dependence on the time interval, we write the (discretised) time interval as

$$\tau/a_\tau = n_1, \dots, N_\tau - n_2, \tag{4.2}$$

where the source is located at $n_1 = 0$ and the maximal time is $N_\tau - 1$, i.e. $n_2 = 1$ (and not $N_\tau/2$). In figure 6 we present the dependence on the final time slice, varying $n_2 = 4, 3, 2, 1$ at a fixed $n_1 = 2$, for $N_\tau = 28$ (left) and 16 (right). Interestingly, we observe a clear double peak structure when the largest possible time is used, $n_2 = 1$. Moreover, the peaks get more pronounced as the temperature is increased. However, the double peak structure is only seen when $n_2 = 1$ and is not robust under variation of n_2. To illustrate this, we show in figure 7 results with $n_2 = 3, 4$ and varying $n_1 = 1, 2, 3, 4$. In this case the output is robust and we recover the spectral functions discussed above. In particular, there is very little dependence on the initial time slice used. While we not fully understand why the inclusion of the entire time interval has this effect, we conclude that the behaviour found when $n_2 = 1$ is anomalous: it presents a thermal lattice artefact due to the periodicity of the gluonic fields through which the b quarks propagate and it should be discarded. For completeness we note that the spectral functions shown in figures 3 and 4 are obtained with $n_1 = 1$ and $n_2 = 3$.

---

[1]Nonsymmetric correlators also appear in the case of thermal Wilson loops, used to construct heavy-quark potentials [27, 28].
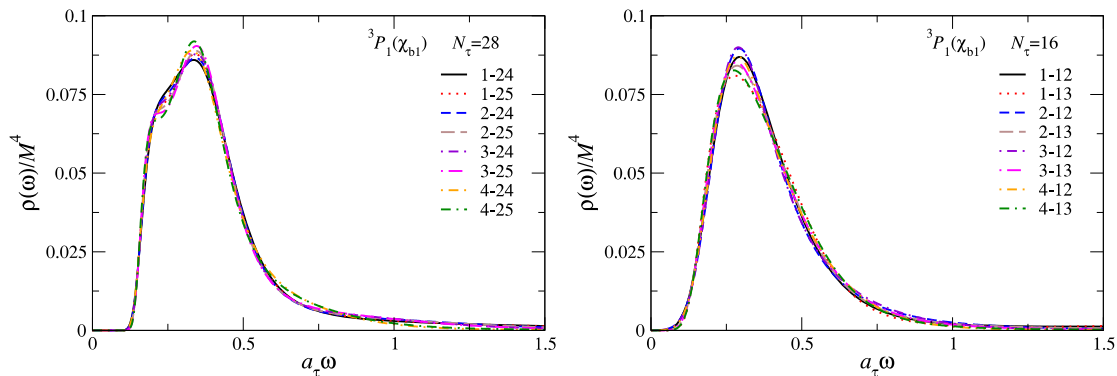
Figure 7. As in figure 6, with $n_1 = 1, 2, 3, 4$ and $n_2 = 4, 3$.

5 Summary

We found strong indications that bottomonium states in the P wave channels (χ_b and h_b) melt in the QGP, at a temperature close to T_c. This is in contrast to the situation in the S wave channels (Υ and η_b) where we found previously that the ground states survive up to the highest temperature we consider, $T/T_c = 2.09$. The conclusion for P waves is based on observations of the correlators and the associated spectral functions, which we find to be consistent: an absence of a plateau in the effective masses in the first case and the absence of an isolated ground state peak in the second. Moreover, above T_c the spectral functions are similar in shape to those found for free nonrelativistic quarks on the lattice. As a technical remark, we note that the MEM results are robust under variation of the euclidean time interval used, provided that the final time slice is not included. We emphasise that our results have been obtained on ensembles with a single lattice spacing: systematic effects related to lattice spacing dependence have not yet been addressed.

As an outlook, we note that there now exist various alternatives to MEM [29, 30] and it would be interesting to apply those techniques in order to gain further confidence in our conclusions, also on ensembles generated with different lattice actions [31]. Similarly, it would be interesting to compare our results with potential model calculations. Finally, we are in the process of extending this work to ensembles with $N_f = 2 + 1$ dynamical quarks, using lattices with an anisotropy of $a_s/a_\tau = 3.5$ and a finer spatial lattice spacing. First results on these $N_f = 2 + 1$ ensembles have been obtained for the electrical conductivity [32] and susceptibilities [33]; the study of bottomonium is currently under investigation [34].

References

[1] T. Matsui and H. Satz, *J/ψ suppression by quark-gluon plasma formation*, *Phys. Lett.* **B 178** (1986) 416 [InSPIRE].

[2] CMS collaboration, *Indications of suppression of excited Υ states in Pb-Pb collisions at* $\sqrt{S_{NN}} = 2.76$ *TeV*, *Phys. Rev. Lett.* **107** (2011) 052302 [arXiv:1105.4894] [InSPIRE].

[3] CMS collaboration, *Observation of sequential Υ suppression in Pb-Pb collisions*, *Phys. Rev. Lett.* **109** (2012) 222301 [arXiv:1208.2826] [InSPIRE].

[4] CMS collaboration, T. Dahms, *Υ suppression in Pb-Pb collisions at the LHC*, PoS(Beauty 2013)021 [arXiv:1307.1795] [InSPIRE].

[5] CMS, ATLAS and ALICE collaborations, A. Rossi, *Heavy-flavour and quarkonia in heavy-ion collisions*, arXiv:1308.2973 [InSPIRE].

[6] A. Mócsy , P. Petreczky and M. Strickland, *Quarkonia in the quark gluon plasma*, *Int. J. Mod. Phys.* **A 28** (2013) 1340012 [arXiv:1302.2180] [InSPIRE].

[7] A. Rothkopf, *From complex to stochastic potential: heavy quarkonia in the quark-gluon plasma*, *Mod. Phys. Lett.* **A 28** (2013) 1330005 [arXiv:1302.6195] [InSPIRE].

[8] J. Ghiglieri, *Review of the EFT treatment of quarkonium at finite temperature*, PoS(Confinement X)004 [arXiv:1303.6438] [InSPIRE].

[9] V. Agotiya, V. Chandra and B. Patra, *Dissociation of 1P quarkonium states in a hot QCD medium*, arXiv:0910.0586 [InSPIRE].

[10] R. Sharma and I. Vitev, *High transverse momentum quarkonium production and dissociation in heavy ion collisions*, *Phys. Rev.* **C 87** (2013) 044905 [arXiv:1203.0329] [InSPIRE].

[11] K. Suzuki, P. Gubler, K. Morita and M. Oka, *Thermal modification of bottomonium spectra from QCD sum rules with the maximum entropy method*, *Nucl. Phys.* **A 897** (2013) 28 [arXiv:1204.1173] [InSPIRE].

[12] C. Dominguez, M. Loewe and Y. Zhang, *Bottonium in QCD at finite temperature*, *Phys. Rev.* **D 88** (2013) 054015 [arXiv:1307.5766] [InSPIRE].

[13] G. Aarts et al., *Bottomonium above deconfinement in lattice nonrelativistic QCD*, *Phys. Rev. Lett.* **106** (2011) 061602 [arXiv:1010.3725] [InSPIRE].

[14] G. Aarts et al., *What happens to the Υ and $η_b$ in the quark-gluon plasma? Bottomonium spectral functions from lattice QCD*, *JHEP* **11** (2011) 103 [arXiv:1109.4496] [InSPIRE].

[15] G. Aarts et al., *S wave bottomonium states moving in a quark-gluon plasma from lattice NRQCD*, *JHEP* **03** (2013) 084 [arXiv:1210.2903] [InSPIRE].

[16] W. Caswell and G. Lepage, *Effective Lagrangians for bound state problems in QED, QCD and other field theories*, *Phys. Lett.* **B 167** (1986) 437 [ɪɴSPIRE].

[17] C. Davies et al., *Precision Υ spectroscopy from nonrelativistic lattice QCD*, *Phys. Rev.* **D 50** (1994) 6963 [hep-lat/9406017] [ɪɴSPIRE].

[18] M. Laine, O. Philipsen, P. Romatschke and M. Tassler, *Real-time static potential in hot QCD*, *JHEP* **03** (2007) 054 [hep-ph/0611300] [ɪɴSPIRE].

[19] Y. Burnier, M. Laine and M. Vepsäläinen, *Heavy quarkonium in any channel in resummed hot QCD*, *JHEP* **01** (2008) 043 [arXiv:0711.1743] [ɪɴSPIRE].

[20] N. Brambilla, M.A. Escobedo, J. Ghiglieri, J. Soto and A. Vairo, *Heavy quarkonium in a weakly-coupled quark-gluon plasma below the melting temperature*, *JHEP* **09** (2010) 038 [arXiv:1007.4156] [ɪɴSPIRE].

[21] N. Brambilla, M.A. Escobedo, J. Ghiglieri and A. Vairo, *Thermal width and gluo-dissociation of quarkonium in pNRQCD*, *JHEP* **12** (2011) 116 [arXiv:1109.5826] [ɪɴSPIRE].

[22] T. Umeda, *A constant contribution in meson correlators at finite temperature*, *Phys. Rev.* **D 75** (2007) 094502 [hep-lat/0701005] [ɪɴSPIRE].

[23] P. Petreczky, *On temperature dependence of quarkonium correlators*, *Eur. Phys. J.* **C 62** (2009) 85 [arXiv:0810.0258] [ɪɴSPIRE].

[24] G. Aarts and J.M. Martínez Resco, *Transport coefficients, spectral functions and the lattice*, *JHEP* **04** (2002) 053 [hep-ph/0203177] [ɪɴSPIRE].

[25] M. Asakawa, T. Hatsuda and Y. Nakahara, *Maximum entropy analysis of the spectral functions in lattice QCD*, *Prog. Part. Nucl. Phys.* **46** (2001) 459 [hep-lat/0011040] [ɪɴSPIRE].

[26] R.K. Bryan, *Maximum entropy analysis of oversampled data problems*, *Eur. Biophys. J.* **18** (1990) 165.

[27] A. Rothkopf, T. Hatsuda and S. Sasaki, *Complex heavy-quark potential at finite temperature from lattice QCD*, *Phys. Rev. Lett.* **108** (2012) 162001 [arXiv:1108.1579] [ɪɴSPIRE].

[28] A. Bazavov and P. Petreczky, *Static meson correlators in $2+1$ flavor QCD at non-zero temperature*, *Eur. Phys. J.* **A 49** (2013) 85 [arXiv:1303.5500] [ɪɴSPIRE].

[29] A. Rothkopf, *Improved maximum entropy analysis with an extended search space*, *J. Comput. Phys.* **238** (2013) 106 [arXiv:1110.6285] [ɪɴSPIRE].

[30] Y. Burnier and A. Rothkopf, *A novel Bayesian approach to spectral function reconstruction*, *Phys. Rev. Lett.* **111** (2013) 182003 [arXiv:1307.6106] [ɪɴSPIRE].

[31] S. Kim, P. Petreczky and A. Rothkopf, *Lattice NRQCD study of in-medium bottomonium states using $N_f = 2+1, 48^3 \times 12$ HotQCD configurations*, PoS(LATTICE 2013)169 [arXiv:1310.6461] [ɪɴSPIRE].

[32] A. Amato et al., *Electrical conductivity of the quark-gluon plasma across the deconfinement transition*, *Phys. Rev. Lett.* **111** (2013) 172001 [arXiv:1307.6763] [ɪɴSPIRE].

[33] P. Giudice et al., *Electric charge susceptibility in $2+1$ flavour QCD on an anisotropic lattice*, PoS(LATTICE 2013)492 [arXiv:1309.6253] [ɪɴSPIRE].

[34] T. Harris et al., *Bottomonium spectrum at finite temperature*, PoS(LATTICE 2013)171 [arXiv:1311.3208] [ɪɴSPIRE].